UNIVERSITAT DE BARCELONA

Field-effects on single molecular circuitry

Electronic transport from synthetic to biological models

Albert Cortijos i Aragonès

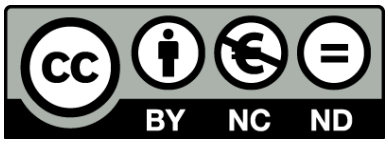

Chapter 4

Chiral inspired biological systems: Peptides

In the previous Chapters 2 and 3 we have seen the spin-dependent selective electron transport on single-molecule devices with asymmetric magnetic junctions given by paramagnetic molecules trapped between a magnetized Ni tip and a Au substrate electrode. Such devices gathered three different asymmetric *key-parameters*, some of them present in the molecular device presented on this Chapter. The molecule-Au bond magnetization ***Spinterface*** is one of these asymmetric *key-parameters* present on previous Chapters to perform spin-dependent transport current measurements. Such effect unbalance the spin-population on the surface as a consequence of a spin-splitting of Au, due the attachment of certain molecules and the polarizing bond established with the Au, as a consequence favors the emission of one specific electron spin and withdraw the other, the effective discrimination between electron polarizations represents the *asymmetry* of the *key-parameter*. This parameter is used again in the single-molecule spin-filer developed on this Chapter. The other asymmetric *key-parameters* employed on this Chapter and also present on the previously presented single-molecule junctions is the Ni electrode ***magnetic polarization***. On the previous studied cases, the main role of this Ni electrode was to tune the MR effect of the junction, orienting the trapped molecule's magnetic moment according to its ***magnetic polarization***. Nevertheless, such polarized electrode had a secondary role because it also controlled indirectly the final device conductance since Ni electrodes select by emit or accept electrons of both orientations with a large energy discrimination between the *minority* and the *majority* spin DOS, resulting as a final selection between spin orientations.[116] That effect did not affect to the switching spin-filter behavior of the previous single-molecule devices because it aligns the molecule, fixing a constant injection of *majority* or *minority* spin-carriers, suppressing the *asymmetry* of the *key-parameter*. But in this Chapter is used this discrimination between the spin-carriers as the Ni tip's main role, in fact represents the second *asymmetry key-parameter*, because allows the current tunning depending on the transmitted spin-carriers through the pretested device.

The new and third asymmetric *key-parameter* is the ***chirality***, which leads the *asymmetry* to the system due the effect explained below, the CISS (Chiral Induced Spin Selectivity). This effect, previously mentioned briefly on ***Section "The role of the Spinterface"*** (Page 96) is based in the electron transport through chiral systems which as a consequence of the interaction with chiral *asymmetry*[339] exhibits noteworthy spin-dependent features without the requirement to have unpaired electrons and molecule spin levels near to the ε_F. The first evidences of this CISS effect on the *nanoscale* appeared on the pioneering work by Naaman and co-workers,[224,340] which shows how in photoemission experiments, electrons are photo-excited from a metal surface and transported through a SAMs of chiral molecules, such processes can be understood under a coherent tunneling with energies above the work function of the material.[224,326,339,508–510] This effect represents a noteworthy analogy to the differential absorption of polarized light by chiral molecules in optical dichroism experiments, for this reason is also known as is called electron dichroism.[349,511–513] The differences between them is that in the former is measured the rotation of the plane of polarization of the electric and magnetic components of the electromagnetic field, whereas in the latter the electronic spin-polarization of the ejected photoelectrons is directly measured.

Electrically the CISS effect can be characterized in electron transport processes applying a bias voltage through the junction and considering the tunneling mechanism keeping the energy below the work function of the material. Reports of such works are few in number, and all of them were based on conductance variations measurements of SAMs employing the AFM technique with a polarized substrate.[514] In this Chapter is presented the first evidence of the CISS effect electrical characterization at the single-molecule scale.

CISS in a molecular junction is considered as a one-electron scattering process[225,339,515,516] due to the molecular electrostatic potential of the chiral structures, resulting in a spin-selective manner which causes the spin-filtering of injected electrons through the chiral molecule and its large SOC.[222–225] Focusing in a SPM measurements, where the electron transport is treated as a one-electron tunneling mechanism and assuming a coherent tunneling as the dominant transport mechanism as well as employing a dimensionless transmission coefficient τ(E,V), under an experimental context where E is the energy of the tunneling electron between two defined electrodes with electrochemical potential of μ_L and μ_R (left and right electrodes, respectively) and V is the applied bias voltage, the adapted simplest Landauer formula version (see *Expression 1.6* on Page 11) is the following:

$$I(V) = \frac{4e}{h} \int_{\mu_R}^{\mu_L} dE\tau(E,V). \tag{4.1}$$

.

For SPM bias voltage's linear regime, usual for single-molecule experiments, the regime is direct tunneling (see *Table 1.1* on Page 14), and *Expression 4.1* becomes:

$$I(V) = \frac{4e^2}{h}\tau(\varepsilon_F)V, \tag{4.2}$$

where, the conductance is given by the Landauer expression:

$$G = \frac{4e^2}{h}\tau(\varepsilon_F), \tag{4.3}$$

and the transmission coefficient $\tau(\varepsilon_F)$ can be written as

$$\tau(\varepsilon_F) = T_{LMR} \cdot g_L(\varepsilon_F) \cdot g_R(\varepsilon_F), \tag{4.4}$$

here T_{LMR} is the effective coupling to the left (L) and right (R) electrodes mediated by a molecule (M) and g represents the densities of states of the L or R electrodes at ε_F. $\tau(\varepsilon_F)$ should be re-written because the incorporation of four spin-polarization effects. Two of them, previously presented on the introduction and already used on previous Chapters 2 and 3, are the ***spin state of the injected electrons*** and the electronic state of the ***DOS contacts***. The other two, are the new incorporated effects related to the transport through chiral molecules: the *(i)* ***chirality*** and the *(ii)* ***helicity*** of the electronic state. The latter is written as the following scalar product:

$$\mu = \frac{s \cdot k}{|k||s|} = \pm 1, \tag{4.5}$$

where s is the spin vector and k is the direction of propagation. Since transmission coefficient obeys symmetry constraints, one should proceed to use an heuristic assumption, in this case *D isomer filters out the negative helicity state* (extract from the experiential results presented later on):

$$\begin{aligned} &\tau_{(D,k,+)} = \tau_{(D,-k,+)}; \tau_{(L,k,-)} = \tau_{(D,-k,-)} \\ &\tau_{(D,k,-)} = \tau_{(L,k,+)} = 0. \end{aligned} \tag{4.6}$$

The first identities correspond to the Kramers doublets and the preservation of time-reversal symmetry in the absence of an external bias. The second one represents the *spin-filtering scenario*, which gives the penalty associated to each chirality's spin preferences. Since the experiments are performed under the presence of an external bias (STM bias voltage), which forces a specific injection direction (*+k* or *-k*), the time-reversal symmetry is broken and the chiral molecule acts as a spin filter in the direction of propagation, thus each chirality can be associated to a specific spin-polarization for the injected electron.

Taking in account all the above concepts, from *Expression 4.4* is obtained the new expression for the spin-dependent transmission coefficient τ_{m_s}:

$$\tau_{m_s} = T_{m_s}^{helix} g_{m_s}^{Au}(\varepsilon_F) g_{m_s}^{Ni}(\varepsilon_F) \left[1 + m_s \frac{\mu_{sN}}{V}\right], \tag{4.7}$$

where the *effective coupling* $T_{\sigma}^{helix}(k)$ is the spin-dependent tunneling matrix element of the peptide related to the spin-orbit interaction (SOC effect) coupled to the

chirality of the helicity,[516] g represents the densities of states of the Au or Ni electrodes at ε_F, m_s (*spin orientation quantum number*) is the factor which implies the double behavior where the selected spin orientation adds a voltage while the other subtracts it, μ_{sN} is a excess chemical potential produced by spin-charge coupling (***Spinterface*** effect), understood as spin-dependent voltage that accelerates electrons of one spin and depends only on the nature of the molecule-surface magnetic interface and V again is the applied bias voltage.[517] Now with the reformulated τ_{m_s} the G expression for the full spin-dependent conductance is the following:

$$G_{m_s} = \frac{4e^2}{h}\tau_{m_s}, \tag{4.8}$$

In summary, the presented theoretical model is based on the modified Landauer transport theory (*Expression 4.7*), where the current dependence is defined by the three mentioned *key-parameters* which will be used to build a new single-molecule device with spin-filtering capabilities. This device will be similar to those previously presented but the ***chirality*** will replace the ***open-shell/molecular paramagnetism*** role employed before, because now instead of using the polarization of the molecule to tune the spin-dependent transport conductance, will be employed the spin preferences of the molecule according its *helicity*[339,515,516] combined along with the ***Spinterface*** and the Ni ***magnetic polarization***.

Since the proposed mechanism for this Chapter is significantly different from the employed on previous Chapters 2 and 3, in the current Chapter the only controlled *key-parameter* was the Ni tip ***magnetic polarization***, because from the other two, the ***open-shell/paramagnetism*** of the molecule depended on the mentioned Ni tip magnetic polarization and the ***Spinterface*** was not tunable. Now, will be controlled two parameters (or subsystems) similarly to a *spin-valve* device: the ***chirality*** and the Ni tip ***magnetic polarization***.

In conclusion, the aim of this Chapter is to study the CISS effect through molecular conductance experiments. To achieve it, was employed the STM technique to develop a single-molecule device and the employed molecules were peptidic structures because they are the best candidates to provide the required chirality to the junction.

4.1 Precedents of peptide charge-transport

In recent years, there have been many works about charge transport using peptides. The first were mainly focused on prove the strong interaction of attached SAMs to metal substrates of α-helical peptides of different *amino acid*-sequences and lengths.[518,519] One of the most representative, demonstrated the capability to orient in a specific way the adsorbed peptides in the used metal substrates. Mainly, was compared the behavior of two different SAMs, one with deprotected SH-terminal and the other with protected SH-terminal.[520] After the addition of colloidal Au-NP they imaged the substrates' surfaces and was observed that a huge number of Au-NP were attached to the deprotected SAM, contrary to the other sample with the protected SAM where practically no nanoparticles were in.[519] Consequence of that work, the Au-S peptide attachment method was used as the basis to link peptides on substrates to allow the electron transfer characterization at the single-molecule level.[518,519,521] Example of that was the work of *Sek* and coworkers, they used this method to prepare SAMs with α-helical peptides of different lengths and determined the electron transfer efficiencies by using a STM-BJ.[519,522] The obtained results showed that the current decayed exponentially with the peptide length, thus revealing a coherent tunneling mechanism, being the first conclusive work about electron transport mechanisms on peptides. Following with the insights about electronic transfer mechanisms, different works[521,523] studied the in *Leu*-based helical peptides of different lengths which contained a electroactive ferrocene (Fc) in the N-terminal. They performed the electrochemical characterization of peptides-SAMs attached in Au micro-electrodes, and through the determination of redox exchange between the Fc group and the electrode surface they determined a tunneling-to-hopping transition as a function of the peptide length. Similarly, Morita *et al.* studied electron hopping processes employing photoelectrons as the first time.[524] The most recent research with peptides and related to spintronics field is the leaded by Naaman and coworkers based on the CISS effects and using photoelectrons.

Nowadays thanks the solid-phase peptide synthesis (SPPS) method pioneered by *R. B. Merrifield*,[525] the peptide synthesizing represents an easy, low-cost and very optimized method which allows the obtention of peptides usually difficult to express in bacteria as well as the incorporation of *amino acids* combined in inexistent way in nature.[525–528] The SPPS technique is based in the use of a solid support in a syringe where *amino acids* are coupled sequentially in elongation-deprotection cycles.[525,527] So one by one, the *amino acids* are linked, N-protected together with other coupling reagents and additives, and always synthesizing the peptide from the C-terminal to the N-terminal.[529,530] During the process, the C-terminal *amino acid* is anchored to an insoluble polymer and the peptide is elongated from de C to N direction by adding *amino acid*-to-*amino acid* according.

4.2 The experimental research

The developed single-molecule device was built employing the STM microscope at RT and the three *ingredients* detailed in the introduction of this Chapter (see Page 217), which were analogous to the asymmetric *key-parameters* of the presented model and allowed the tunning of the single-molecule junction conductance. The ***chirality*** of the system was controlled employing asymmetric "model" molecules(i) as the first *ingredient*. Such molecules were two synthesized α-peptides series of 17 and 22-*amino acid units* (AA) following reported protocols.[529,531,532] Both series of peptides presented Dextrorotatory (D-) and Levorotatory(L-) chiral isomers. The tunning of ***magnetic polarization*** was defined by using the second *ingredient*, the *ex-situ* magnetized Ni STM tips(ii) in ↑Ni or ↓Ni directions along the main junction axis using the Au substrate as a reference. Finally, the polarization of the molecule-surface due the ***Spinterface***,[327–329] being the only inherent and experimentally non-tunable factor, the only requirement was use Au as material for the substrate electrodes(iii) because as has been proved is the unique chemical element that allows an effective spin-polarization of the surface and therefore spin-dependent transport. The other required component to establish an effective ***Spinterface*** via a strongly polarized bond with Au is the use of -S terminus *anchoring groups*,[326,328,329,336,341] for the explained reasons in ***Section "The role of the Spinterface"*** (Page 96) The peptides' -S terminus found at both sides of the chain as *anchoring groups*, belong to the free thiol (-SH) group at the C-terminus (cysteamine linker) and to the terminal of Cys residues. Another controlled parameter but no related to the *key-parameters* of the model, was the applied bias voltage parameter used to control the current direction being positive for the *Ni tip-to-Au substrate* current sense and negative for *Au substrate-to-Ni tip current* sense. Figure 4.1 summarizes the three *ingredients* gathered to carry out the experiments.

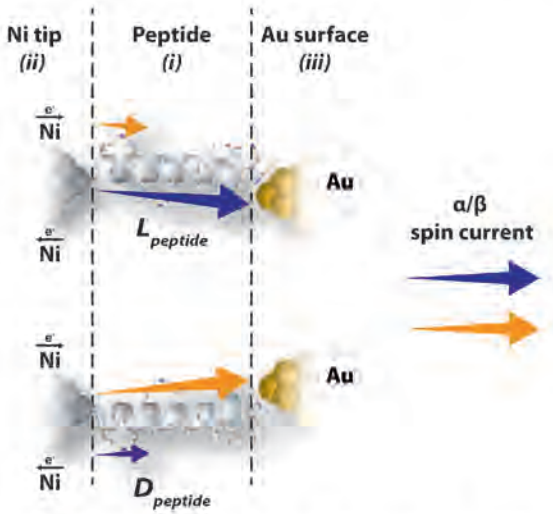

Figure 4.1: Schematic representation of the single-molecule device showing spin-filtering capabilities with the three "ingredients" labeled.

In this occasion was employed the STM-BJ technique (see *Section "STM Break-Junction Technique"*, on Page 26) as a tested robust and stable molecular attachment into its dynamical *tapping* approach (see *Appendix C.1*, Page 325 for a detailed explanation), to obtain robust statistics of the detected single-molecule current signatures from thousands of performed junctions, of individual peptide molecules trapped between the tip electrode and the Au substrate under the different experimental conditions detailed above. The STM experiments were carried out employing polycrystalline Ni wire to obtain the STM tips electrodes and Au(111) monocrystals were utilized as substrate electrodes, the used medium was a polar organic mixture of TFE/H_2O:(60/40 v/v) to keep the structural helicity.[533] A detailed description of the sample, substrate and tip preparation can be found from Page 328 (*Appendix C.2*).

4.3 Objectives and Summary of the experimental work

- In order to evaluate the preservation of the α-helical conformation of the target peptides under the described STM set-up, the β decay factor was required to be determined and compared with previously reported similar peptide structures.[313,534] To obtain such information, were measured peptides of different length, D-α-17AA-peptides and D-α-22AA-peptides. The single-current measurements were performed under +50 mV of bias voltage and employing non-magnetized electrodes using Au tips and substrate electrodes.

- Under non-polarized electrodes (Au tips and substrate electrodes) the single-current measurements of D- and L-α-22AA-peptides were measured to validate the *helicity* selection effect under non-polarized current. The applied bias voltage values were -50 mV and +50 mV (same magnitude but different current sense).

- To study the spin-dependent current response on the established singe-molecule device, the experiments were conducted employing the three combined essential experimental variables, both Ni tip magnetic polarization directions ↑Ni and ↓Ni, L and D chiralities of α-22AA-peptides and the current sense applying same bias voltage magnitudes but different in polarity, -50 mV and +50 mV.

In the following pages is shown summarized the research as a published paper and its Supplementary Information:

"Albert C. Aragonès, Ernesto Medina, Miriam Ferrer-Huerta, Nuria Gimeno, Meritxell Teixidó, Julio L. Palma, Nongjian Tao, Jesus M. Ugalde, Ernest Giralt, Ismael Díez-Pérez, and Vladimiro Mujica. Measuring the Spin-Polarization Power of a Single Chiral Molecule. *Small*, 13(2):1602519, jan 2017".

Materials Views
www.MaterialsViews.com

NANO MICRO small

Chiral Transport

Measuring the Spin-Polarization Power of a Single Chiral Molecule

Albert C. Aragonès, Ernesto Medina, Miriam Ferrer-Huerta, Nuria Gimeno, Meritxell Teixidó, Julio L. Palma, Nongjian Tao, Jesus M. Ugalde, Ernest Giralt,* Ismael Díez-Pérez,* and Vladimiro Mujica**

Electron transport in chiral systems exhibits a number of remarkable features having to do with the fact that spin–orbit interaction induces a coupling between the linear momentum and the spin of electrons, which translates into the appearance of spin polarization and spin filtering. The phenomenon is called electron dichroism as, in many ways, it is the equivalent of the better-known optical dichroism effect. In the latter, it is the rotation of the plane of polarization of the magnetic and electric components of the electromagnetic field that is experimentally measured, whereas the former corresponds to the polarization of the electronic spin. The phenomenon is also known as chirality-induced spin selectivity (CISS),[1] inferring that the transport of one of the electronic spins is facilitated over the other in a chiral structure.

In its simplest description, CISS in a molecular junction can be considered as a one-electron scattering process due to the molecular electrostatic potential of the chiral structure. In photoemission experiments, electrons are photoexcited from a metal surface and transmitted through a self-assembled monolayer of chiral molecules;[2] whereas in the case of local scanning probe microscopies (SPM), there is a transport process of electrons under a bias voltage through the junction.[3] Both experimental situations, photoemission and SPM, can be thought of as tunneling processes with energies above or below the work function of the material, respectively. In photoemission experiments, the spin polarization of the ejected electrons has been directly measured, and it has been found that very large polarization factors can be obtained starting with an unpolarized electron state.[2] In the case of SPM measurements, the manifestation of spin polarization is a change in the observed conductance, e.g. measurable spin-dependent threshold voltage of the charge transport through the junction.[3]

In this article, we report on a striking experimental manifestation of CISS in a single-molecule scanning tunneling microscopy (STM) break-junction, consisting of individual peptide molecules of well-defined chirality bridged between a magnetized STM Ni tip and an Au electrode. These experiments constitute the first reported case of observed current asymmetries in single chiral molecular junctions using the STM break-junction technique, where the statistics of many single-molecule measurements are collected and represented in a conductance histogram. It is important to mention, in this context, the pioneering work by Naaman and co-workers, which showed, using a completely different

A. C. Aragonès, M. Ferrer-Huerta, N. Gimeno, Prof. I. Díez-Pérez
Department of Material Science and Physical Chemistry
University of Barcelona
Barcelona, 08028 Catalonia, Spain
E-mail: isma_diez@ub.edu

A. C. Aragonès, Prof. I. Díez-Pérez
Institute for Bioengineering of Catalonia (IBEC)
Barcelona, 08028 Catalonia, Spain

A. C. Aragonès, Prof. I. Díez-Pérez
Centro Investigación Biomédica en Red (CIBER-BBN)
Campus Río Ebro-Edificio I+D
Poeta Mariano Esquillor s/n, 50018 Zaragoza, Spain

Prof. E. Medina
Centro de Física
Instituto Venezolano de Investigaciones Cientificas (IVIC)
Apartado 21827, Caracas 1020A, Venezuela
E-mail: ernesto@ivic.gob.ve

Prof. E. Medina
School of Physics Yachay Tech
Yachay City of Knowledge
100119 Urcuqui, Ecuador

DOI: 10.1002/smll.201602519

Dr. M. Teixidó, Prof. E. Giralt
Institute for Research in Biomedicine (IRB Barcelona)
Barcelona Institute of Science and Technology (BIST)
Baldiri Reixac 10, 08028 Barcelona, Spain
E-mail: ernest.giralt@irbbarcelona.org

Dr. J. L. Palma, Prof. N. Tao, Prof. V. Mujica
Arizona State University School of Molecular Sciences
Physical Sciences Center PSD-D102 and Biodesign
Institute Center for Bioelectronics and Biosensors
Tempe, AZ 85287, USA
E-mail: vmujica@asu.edu

Prof. J. M. Ugalde, Prof. V. Mujica
Donostia International Physics Center (DIPC)
Manuel Lardizabal Ibilbidea, 4, 20018 Donostia, Gipuzkoa, Spain

Prof. E. Giralt
Departament de Química Orgánica
Universitat de Barcelona
Barcelona, 08028 Catalonia, Spain

junction architecture, that nanoscale molecular junctions formed by trapping few DNA molecules between an Au nanoparticle and an Ni ferromagnetic surface display current asymmetries as a function of the direction of the Ni magnetic polarization.[3]

The control of two experimental variables, the magnetization orientation of the Ni tip and the chirality of the peptide, allows probing the three key physical asymmetries of the junction regulating its conductance: magnetoresistance, chirality, and spinterface (interfacial magnetism arising as a result of the metal/molecule interaction), and they allow us to extract a value of the spin-polarization power (capability to spin-polarize electrical current) of a single chiral molecule of ≈60%. These experiments can be understood and rationalized in terms of a theoretical model that connects spin polarization with transport in molecular junctions recently developed by Medina and co-workers, which generalizes the well-established Landauer model for electron transport in metal–molecule–metal junctions to include the filtering effect of the molecular chirality and the presence of a magnetized electrode.[4,5]

The combined theoretical and experimental analysis affords a novel way to estimate the molecular spin-polarization power, which is essentially the spin-dependent transmission probability, a magnitude that is directly linked to the single-molecule conductance.

We have measured the spin-dependent single-molecule conductance of an α-helical peptide sequence of 22 amino acid (AA) residues of both L- and D-isomers (see **Figure 1**), employing a spin-polarized version[8] of the STM break-junction approach.[6–8] The procedure is based on driving a magnetically polarized STM Ni tip in and out of contact to/from an Au(111) substrate functionalized with the target peptide immersed in a helical-inducing liquid medium (TFE(2,2,2-Trifluoroethanol)/H_2O: 60/40 v/v[9]). During the contact process, individual peptides can spontaneously bridge between both biased electrodes via two –S terminal groups (see Figure 1).[10] The current was recorded for each pulling stage in the form of current versus time/displacement, and all traces

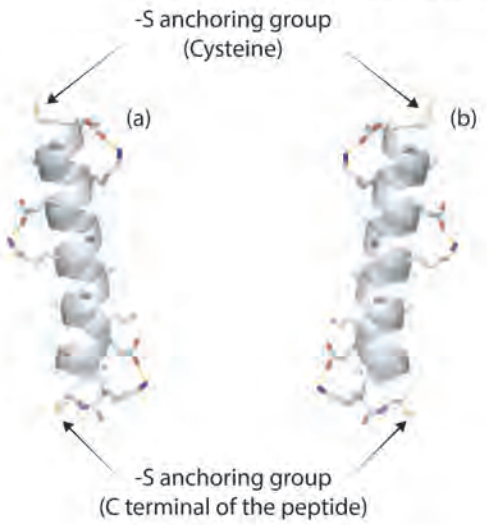

Amino acid sequence:
H-CEAAAKEAAAKEAAAKEAAAK-NH-CH_2-CH_2-SH

Figure 1. Secondary structure of the dextrorotatory (D-) (a), and levorotatory (L-) (b) α-22AA-peptides and the amino acid sequence synthesized in this work.

displaying well-defined single-molecule plateau features (see **Figure 2**) were used to build a conductance histogram.[6] The observed maxima represent the most probable conductance values for the formed single-molecule contact (see Section S6 in the Supporting Information for more details).

In the single-peptide transport measurements, we focus on the three key physical parameters of our model (Figure 2): (1) the chirality of the molecular backbone, which

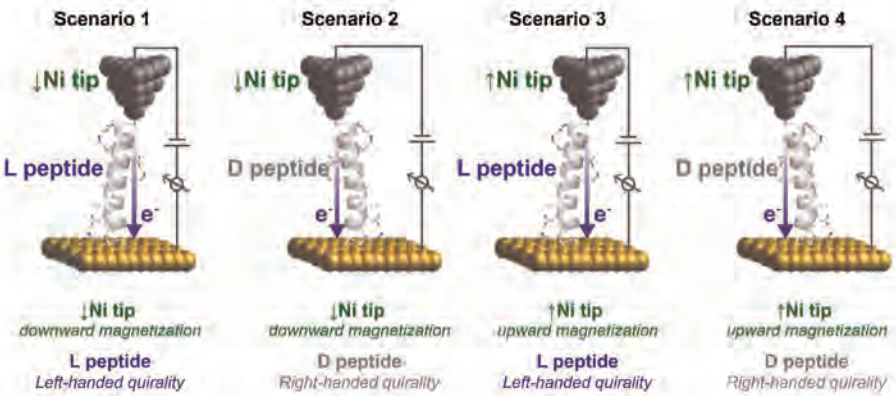

Figure 2. Schematic representation and description of the four studied case scenarios combining the three key experimental parameters. Sample bias voltage (defined as sample minus tip voltages) is positive meaning the electrons are flowing from the Ni to the Au electrodes.

small 2016,
DOI: 10.1002/smll.201602519

Materials Views
www.MaterialsViews.com
small NANO MICRO

is introduced by measuring the D- and L-enantiomers (for synthetic details see Supporting Information, Section S5); (2) the initial polarization state, which is defined by using premagnetized Ni STM tips in both directions along the main junctions' axis; and (3) inherent magnetization at the molecule/electrode interface due to the strongly polarizing nature of the Au–S bond (spinterface).[8,11–13]

We present here the results of the four case scenarios where the electrons are injected from the Ni-polarized source into the chiral peptide backbone and drained through the bottom Au electrode (see Figure 2). These cases are the most representative ones of the observed spin-dependent transport through the chiral molecular structures. The four cases corresponding to the opposite bias voltage (current being injected from the nonmagnetic Au bottom electrode) also show spin-dependent transport effects and they are analyzed in the Supporting Information (section S2) within the same model framework. The single-peptide conductance histograms in **Figure 3**a,b show that when the magnetic polarization of the Ni tip is reversed, the conductance for the D- and L-isomers switch the order, being the highest and the lowest conductance sets for the L- and D-isomers, respectively, both under "spin-up Ni magnetization direction". These experimental observations will be contrasted to the different scenarios described within the framework of our model below.

We have developed a theoretical model for the description of CISS, which clearly establishes that this phenomenon is the result of the combined effect of broken space inversion symmetry due to chirality, spin–orbit interaction, and broken time reversal symmetry by an external bias that selects a preferential direction for electron injection (see related experimental results in the Supporting Information, Section S2). These conditions are satisfied in all instances of experimental setups where CISS has been observed, i.e., electron photoemission, electron transport in molecular junctions, and intramolecular electron transfer.[2,3,14]

In presenting the simplest version of a theoretical model that accounts for a quantitative interpretation of the experimental results we need to explicitly connect spin polarization with conductance. To this end, we consider that electron transport occurs via a one-electron tunneling mechanism under the Landauer regime, where the current is well described by a dimensionless transmission coefficient $\tau(E,V)$, which depends on the nature of the tunneling barrier (see experimental assessment on the transport mechanisms in Supporting Information, Section S1)

$$I(V)=\frac{4e}{h}\int_{\mu_L}^{\mu_R} \mathrm{d}E\tau(E,V) \tag{1}$$

where E is the energy of the tunneling electron, V is the applied bias voltage, and μ_L and μ_R are the electrochemical potentials in the left and right electrodes, respectively. In the linear regime of low bias voltage, which is the one we will be concerned with here, Equation (1) becomes

$$I(V)=\frac{4e^2}{h}\tau(E_F)V \tag{2}$$

In this regime, the conductance is given by the Landauer expression

$$G=\frac{4e^2}{h}\tau(E_F) \tag{3}$$

where the transmission coefficient can be written as

$$\tau(E_F)=T_{LMR}g_L(E_F)g_R(E_F) \tag{4}$$

and T_{LMR} is the effective coupling to the left (L) and (R) electrodes mediated by the molecule M and $g_{L/R}(E_F)$ are the densities of states of the L/R electrodes at the Fermi energy. The effective coupling is a product of the term connected to the propagation of electrons through the molecule, and the coupling of the molecule to the electrodes.

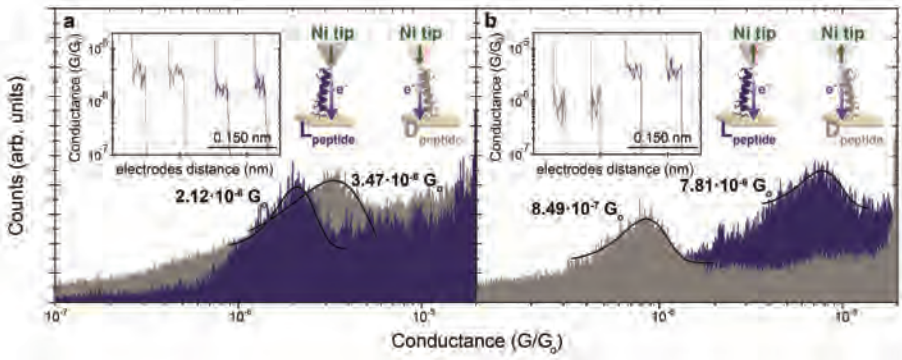

Figure 3. Semilog conductance histograms (counts vs G/G_0, G_0 being the conductance quantum equal to 77.5 μS) for the dextrorotatory and levorotatory α-22AA-peptides under spin down a) and up b) Ni magnetic polarizations. The short green arrows indicate the Ni-tip magnetization direction while the violet arrows indicate the electron injection direction. The conductance values were extracted from Gaussian fits from the histogram peaks. The applied sample bias was set to +50 mV. Insets show representative current versus pulling traces used to build the conductance histograms.

DOI: 10.1002/smll.201602519

In the presence of spin-polarization effects, Equation (4) has to be modified in several ways. First, the transmission coefficient needs to include information about the spin state of the electrons entering the junction. Second, an explicit dependence on the chirality of the molecule must be included. Third, an explicit indication of the helicity of the electronic state must be given. The helicity of an electronic state is specified by the projection of the spin vector in the direction of propagation, i.e., by the scalar product $s \cdot k/(|k||s|) = \pm 1$. Fourth, the contact density of states (DOS) also depends on spin in a way that will be specified below. We include this information by adding three subindices to the notation for the transmission coefficient, i.e., $\tau_{M,\mathbf{k},\mu}$, where the molecular index M can take the values D and L; k indicates the propagation direction; and $\mu = \pm 1$ is the helicity index.

We have shown that the transmission coefficient obeys the important symmetry constraints, assuming that the D isomer filters out the negative helicity state

$$\begin{aligned} &\tau_{D,\mathbf{k},+} = \tau_{D,-\mathbf{k},+};\ \tau_{L,\mathbf{k},-} = \tau_{L,-\mathbf{k},-} \\ &\tau_{D,\mathbf{k},-} = \tau_{L,\mathbf{k},+} = 0 \end{aligned} \tag{5}$$

where the first relations correspond to the Kramers doublets and the preservation of time-reversal symmetry in the absence of an external bias, and the second relations represent the filtering conditions, i.e., a high handicap to transport for the filtered out spin component. The essential physical content of these relations is that chiral molecules are filters of electronic state helicity rather than electronic spin.

In the presence of an external bias, which forces a specific injection direction, either +k or –k, time-reversal symmetry is broken and the chiral molecule acts as a spin filter in the direction of propagation, i.e., each optical isomer selects an electron spin polarization (fixed by helicity).

The conductance through the peptide from the Ni to the Au contact is controlled by two factors according to Equation (4): the product of the densities of states of each contact $g_{m_s}^{Au,Ni}(\varepsilon_F)$ evaluated at the Fermi level for either the Au or the Ni, where m_s denotes the spin orientation quantum number, and the effective coupling $T_{\sigma}^{helix}(k)$, which is the spin-dependent tunneling matrix element of the peptide. In addition to the tunneling process through the molecule and the density of states at the contacts, there is an interfacial magnetic effect that in practice imposes an energy penalty to polarized electrons. A specific model of this phenomenon, referred to as spinterface, has been extensively used.[8,15] Such a coupling produces a spin-dependent bias voltage that changes the effective conductance of the molecular junction. This effect is small compared to the molecular filtering properties and the DOS spin-imbalance at the Fermi energy of the magnetic contact; however, it must be included to fully describe the experimental observations.

We now write the full spin-dependent conductance as

$$G_{m_s} = \frac{4e^2}{h}\tau_{m_s} \tag{6}$$

where the spin-dependent transmission coefficient is given by

$$\tau_{m_s} = T_{m_s}^{helix} g_{m_s}^{Au}(\varepsilon_F) g_{m_s}^{Ni}(\varepsilon_F)\left[1 + m_s \frac{\mu_{sN}}{V}\right] \tag{7}$$

where μ_{sN} is the excess chemical potential produced by spin–charge coupling between the Au substrate and the anchoring group, V is the applied voltage to the Au contact, and the m_s factor implies that one spin orientation adds a voltage while the other subtracts it. μ_{sN} is a spin-dependent voltage that accelerates electrons of one spin, and it does not depend on the chirality of the molecule but only on the nature of the magnetic interface.[8,16] The associated voltage to the spin–charge coupling favors injecting spin up into the molecule, while by the same token favors withdrawing spin down from the molecule.

Equation (6) is a fundamental result connecting, in an explicit way, spin polarization and conductance. In fact, it allows estimating the spin-polarization power of a molecule, the analog of the optical rotational power in photon dichroism, by simply dividing the conductances corresponding to the two optical isomers in a chiral junction. This aspect of the theoretical model will be further explored in a forthcoming publication.

Regarding the $T_{\sigma}^{helix}(k)$ according to the theory,[17] the spin–orbit interaction coupled to the chirality of the helix generates a gap between two Kramers doublet states (four states combining two propagation directions and two spin orientations) with well-defined helicity.[4,5] We consider that, in our experiments, the electronic state helicity (spin) is strongly selected through this mechanism.

Regarding the DOS of the metallic contacts, in the case of Au, there is no discrimination according to the electron spin, so Au emits or accepts electrons of both orientations equally well except for the extra spin–charge voltage described by μ_{SI} due to the anchoring group. On the other hand, Ni displays a large contrast between the minority and the majority spin DOS.[18] According to the DOS of nickel, there is a handicap for injecting or emitting the majority spin as compared to the minority spin. With these ingredients we can understand the results shown in Figure 3.

Figure 4 summarizes, within the frame of previous arguments, the conductance hierarchy according to favorable/unfavorable transmitted electron spin toward the chiral peptide or the spin–charge voltage. The corresponding experimental values of the conductances (Figure 3) have been organized in ascending values in the bottom X-axis. The Ni electrode is assumed to inject minority spin electrons in the junction according to its spin-polarized DOS distribution near the Fermi level. The helicity state chosen by the chiral molecule is that L-isomers (D-isomers) carry positive (negative) helicity. One can readily see that the two higher conductances correspond to the preferred spin by the peptide, being the larger conductance value the one that sees the preferred spin for the spin–charge effect as well. The two smaller conductances correspond to the unfavorable directions for the chiral peptide, again in order of preference of the spin–charge effect. With these results, we can disentangle the larger chiral effect in the spin-dependent transport of these single-peptide junctions versus the spinterface effect due to the spin–charge voltage. For the case of the current in the Au to Ni direction, the conductance hierarchy can be understood in the same terms (see Supporting Information, Section S2).

small 2016,
DOI: 10.1002/smll.201602519

Materials Views
www.MaterialsViews.com
NANO MICRO small

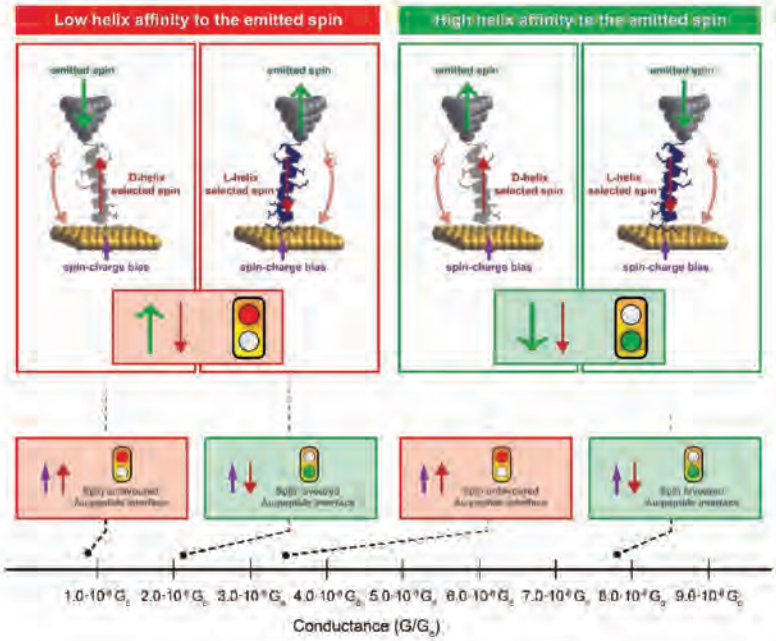

Figure 4. Transport of electrons from the Ni to the Au electrodes. We order the experimental values of the conductance in the X axis, increasing to the right. The binary lights signal the resistance to electron transfer; green is the lower and red is the higher resistor as described in the text. The D peptide supports negative helicity (spin antiparallel to current sense) while the L peptide supports positive helicity transport (spin parallel to current sense). The central light refers to the electron helicity selected by the chiral molecule, while the small bottom light refers to the spin–charge voltage effect, which always favors down spin versus up spin when injected to the Au.

A straightforward application of the above-mentioned conceptual framework allow us to calculate the polarization power for each isomer (L or R) as the asymmetry factor between the currents flowing through the same isomer for the two opposite Ni electrode magnetic polarizations

$$SP_{L/R}\,(\%) = \frac{G^{>}_{L/R} - G^{<}_{L/R}}{G^{>}_{L/R} + G^{<}_{L/R}} \qquad (8)$$

where $G^{>}$ and $G^{<}$ are the high and low conductance levels for each isomer. A simple calculation yields $SP_L = 60\%$ and $SP_D = 57\%$, which are remarkably similar within the experimental accuracy. Theoretically, one should also expect similar results since the symmetry breaking and spin–orbit effects responsible for the phenomenon are molecular in origin. It is interesting to notice that these values are comparable to those measured in electron photoemission experiments with DNA for much larger chains.[2] This raises the unresolved question as to whether the spin-polarization effect for transport at energies above and below the work function is the result of purely coherent process (tunneling) or includes an incoherent mechanism (hopping).

The helicity preference is contemplated by the theory elsewhere.[4,5,17] A source of asymmetry not explicitly discussed, nevertheless, is the direction of the always-present dipole moment along the oligopeptide axis. Eckshtain-Levi et al.[19] have shown that one indeed reverses the selected spin by reversing the molecule (e.g., oligopeptides based on alanine[20]). This result comes most likely from the difference in electron affinity between the molecule and the gold surface generating a net charge transfer and a large fixed electric dipole for all the configurations studied. In terms of the model, the dipole could make the Rashba term larger than the intrinsic spin–orbit interaction and yield a dipole orientation-dependent filter. This is an issue for further study.

In summary, we have established, for the first time, a direct verification of the spin filtering capabilities of chiral molecules using a break-junction STM technique, in an asymmetric magnetic single-molecule junction, consisting of a magnetized Ni tip, a Au electrode, and a chiral molecule. The results are strikingly consistent with a modified Landauer transport theory that takes into account the properties of the magnetic contact, the helicity selection of the chiral filter, and the interfacial effects induced by chemical bonding. The theoretical model is capable of explaining the experimental results for the eight different scenarios determined by the variation in the three control variables: the direction of the voltage in the junction, the spin selection of the chiral molecule, and the polarization of the Ni tip.

The strong rectification effects observed in the limit of zero voltage conductance confirm the molecular nature of the spin filtering effect, even in the absence of the electric field associated with the bias, and the huge potential of

DOI: 10.1002/smll.201602519

www.MaterialsViews.com

chiral filters as circuit components in spintronics devices. They also offer an experimental glance at a deep connection between spin polarization and tunneling transmission, which affords a direct assessment of the molecular spin-polarization power, a topic that we will address in depth in a forthcoming publication.

The implications of our findings for the general field of electron transport through chiral media are considerable, especially in the field of electron transfer in biological systems, because the same physical mechanism responsible for the spin-induced rectification effects in the junction underlie the fact that spin polarization provides for a mechanism to lower the transmission tunneling barriers in molecules.

Supporting Information

Supporting Information is available from the Wiley Online Library or from the author.

Acknowledgements

This research was supported by the MINECO Spanish National Projects (Grant Nos. CTQ2015-71406-ERC, CTQ2015-64579-C3-3-P, BIO2013-40716-R, and CTQ2013-49462-EXP) and Generalitat de Catalunya (XRB, 2014-SGR-1251, and 2014-SGR-521). V.M. acknowledges the generous support of the Donostia International Physics Center during his Sabbatical Year. V.M. is grateful to Prof. Mark Ratner for inspiring discussions about the subject. E.M. acknowledges Dr. Werner Bramer for useful observations. I.D.-P. thanks the Ramon y Cajal program (MINECO, No. RYC-2011-07951) for financial support. A.C.A. thanks the Spanish Ministerio de Educación for an FPU fellowship. IRB Barcelona and IBEC are recipients of a Severo Ochoa Award of Excellence from MINECO (Government of Spain).

[1] S. G. Ray, S. S. Daube, G. Leitus, Z. Vager, R. Naaman, *Phys. Rev. Lett.* **2006**, *96*, 36101.
[2] B. Göhler, V. Hamelbeck, T. Z. Markus, M. Kettner, G. F. Hanne, Z. Vager, R. Naaman, H. Zacharias, *Science* **2011**, *331*, 894.
[3] Z. Xie, T. Z. Markus, S. R. Cohen, Z. Vager, R. Gutierrez, R. Naaman, *Nano Lett.* **2011**, *11*, 4652.
[4] S. Yeganeh, M. A. Ratner, E. Medina, V. Mujica, *J. Chem. Phys.* **2009**, *131*, 14707.
[5] E. Medina, F. López, M. A. Ratner, V. Mujica, *EPL* **2012**, *99*, 17006.
[6] B. Xu, N. J. Tao, *Science* **2003**, *301*, 1221.
[7] N. J. Tao, *Nat. Nanotechnol.* **2006**, *1*, 173.
[8] A. C. Aragonès, D. Aravena, J. I. Cerdá, Z. Acís-Castillo, H. Li, J. A. Real, F. Sanz, J. Hihath, E. Ruiz, I. Díez-Pérez, *Nano Lett.* **2016**, *16*, 218.
[9] B. P. Orner, X. Salvatella, J. Sánchez Quesada, J. De Mendoza, E. Giralt, A. D. Hamilton, *Angew. Chem. Int. Ed. Engl.* **2002**, *41*, 117.
[10] S. Sek, K. Swiatek, A. Misicka, *J. Phys. Chem. B* **2005**, *109*, 23121.
[11] S. Trudel, *Gold Bull.* **2011**, *44*, 3.
[12] A. Hernando, P. Crespo, M. A. García, E. F. F. Pinel, J. de la Venta, A. Fernández, S. Penadés, M. A. Garcia, A. Fernandez, S. Penades, *Phys. Rev. B* **2006**, *74*, 52403.
[13] R. Gréget, G. L. Nealon, B. Vileno, P. Turek, C. Mény, F. Ott, A. Derory, E. Voirin, E. Rivière, A. Rogalev, F. Wilhelm, L. Joly, W. Knafo, G. Ballon, E. Terazzi, J.-P. Kappler, B. Donnio, J.-L. Gallani, *ChemPhysChem* **2012**, *13*, 3092.
[14] P. C. Mondal, C. Fontanesi, D. H. Waldeck, R. Naaman, *ACS Nano* **2015**, *9*, 3377.
[15] F. Al Ma'Mari, T. Moorsom, G. Teobaldi, W. Deacon, T. Prokscha, H. Luetkens, S. Lee, G. E. Sterbinsky, D. A. Arena, D. A. MacLaren, M. Flokstra, M. Ali, M. C. Wheeler, G. Burnell, B. J. Hickey, O. Cespedes, *Nature* **2015**, *524*, 69.
[16] J. Fabian, A. Matos-Abiague, C. Ertler, P. Stano, I. Žutić, *Acta Phys. Slovaca. Rev. Tutorials* **2007**, *57*, 342.
[17] S. Varela, V. Mujica, E. Medina, *Phys. Rev. B* **2016**, *93*, 155436.
[18] E. Tsymbal, *Handbook of Spin Transport and Magnetism*, Chapman & Hall/CRC: Boca Raton, FL, USA **2011**.
[19] M. Eckshtain-Levi, E. Capua, S. Refaely-Abramson, S. Sarkar, Y. Gavrilov, S. P. Mathew, Y. Paltiel, Y. Levy, L. Kronik, R. Naaman, *Nat. Commun.* **2016**, *7*, 10744.
[20] I. Carmeli, V. Skakalova, R. Naaman, Z. Vager, *Angew. Chem. Int. Ed. Engl.* **2002**, *41*, 761.

Received: July 28, 2016
Revised: September 8, 2016
Published online:

DOI: 10.1002/smll.201602519

Supporting Information

Measuring the Spin-polarization Power of a Single Chiral Molecule

Albert C. Aragonès[1,2], Ernesto Medina[3,4*], Miriam Ferrer-Huerta[1], Nuria Gimeno[1], Meritxell Teixido[5], Julio L. Palma[6], Nongjian Tao[6], Jesus M. Ugalde[7], Ernest Giralt[5,8*], Ismael Díez-Pérez[1,2*], Vladimiro Mujica[6,7*]

[1]Department of Material Science and Physical Chemistry, University of Barcelona, Barcelona 08028, Catalonia, Spain.
[2]Institute for Bioengineering of Catalonia (IBEC), Barcelona 08028, Catalonia, Spain and Centro Investigación Biomédica en Red (CIBER-BBN). Campus Río Ebro-Edificio I+D, Poeta Mariano Esquillor s/n, 50018 Zaragoza, Spain.

[3]Centro de Física, Instituto Venezolano de Investigaciones Cientificas (IVIC), Apartado 21827, Caracas 1020A, Venezuela.
[4]School of Physics Yachay Tech, Yachay City of Knowledge, 100119-Urcuqui, Ecuador.
[5]Institute for Research in Biomedicine (IRB Barcelona), Barcelona Institute of Science and Technology (BIST), Baldiri Reixac 10, 08028 Barcelona, Spain.
[6]Arizona State University, School of Molecular Sciences Physical Sciences Center PSD-D102 and Biodesign Institute Center for Bioelectronics and Biosensors, Tempe, AZ 85287, U.S.A
[7]Donostia International Physics Center (DIPC) Manuel Lardizabal Ibilbidea, 4, 20018 Donostia, Gipuzkoa, Spain
[8]Departament de Química Orgánica, Universitat de Barcelona, Barcelona 08028, Catalonia, Spain.

Index

1. Length dependence single-molecule transport measurements

We first characterized the length dependence of the conductance for the studied α-helical sequence. The extracted beta decay factor (β) is then compared to those previously reported for similar peptidic conformations in order to assess the preservation of the α-helical conformation in the single-molecule junction. To this aim, we have built single-molecule conductance histograms for both D-17 and D-22AA α-helical sequences (Fig. 1a-b). Both histograms display conductance features at $2.1 \cdot 10^{-5}$ G_o and $2.8 \cdot 10^{-6} G_o$ respectively, from where it is possible to estimate a decay factor β of 2.7 nm^{-1}. It is useful to compare this value with β values of other previously measured molecular backbones, for example, for simple saturated alkane chains, typical values above 8 nm^{-1} have been reported[1], while the introduction of conjugated π-orbital systems or the transport transition to a hopping regime drops these values down to 0.5 nm^{-1} [2,3]. The conductances and beta values obtained here are comparable to those previously reported for similar systems,[4,5] and it suggests coherent tunneling as the dominant transport mechanism through the α-helical sequence.

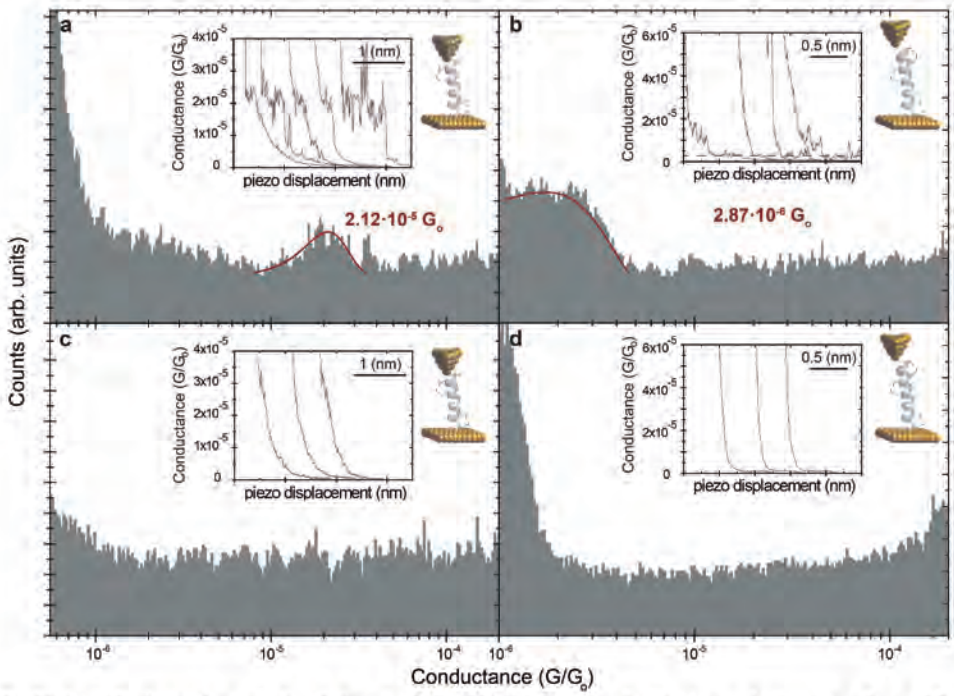

Fig.S1 Length dependent study of the single-peptide transport. Conductance histograms for a 17 AA peptide (2.55 nm) (a) and a 22 AA peptide (3.3 nm)(b). The peptide lengths are taking from a chemical model (Chemdraw optimization). (c,d) Control experiments on the corresponding thiol-protected peptides bearing a protecting group at the thiol group of distal cysteine residue, which prevents the peptide to efficiently connect to the top gold electrode. Sample bias voltage was set to +50 mV. In all cases, a Au-molecule-Au junction were built.

2. Additional single-molecule transport measurements

2.1 Non-polarized transport

As a control experiment, we have measured the single-molecule conductance of the two optical isomers of the α-22AA-peptide (Fig. S2.1). The single-molecule conductance in both cases is experimentally undistinguishable in agreement with the use of non-polarized source and drain electrodes. The helicity selection effect in the helical structure for the electrons injected from the Au non-polarized source is now undetectable by the non-polarized drain Au electrode.

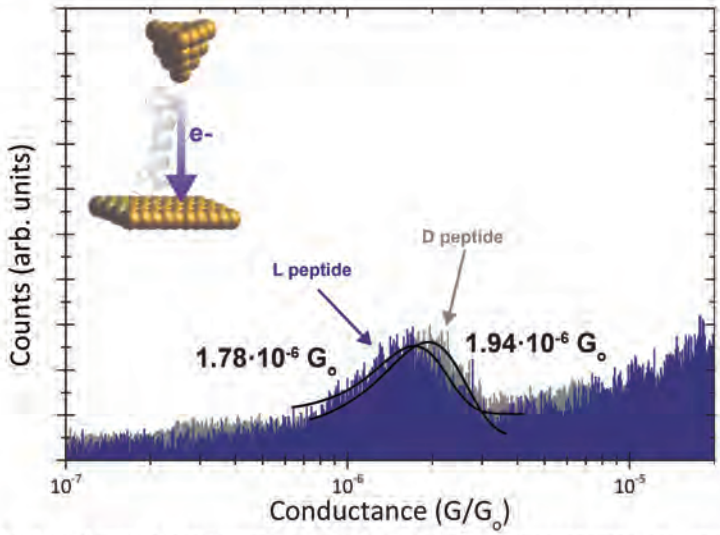

Fig.S2.1 Semilog conductance histograms for the dextrorotatory and levorotatory α-22AA-peptides, under a positive sample bias voltage of +50 mV using a non-magnetic Au tip.

2.2 Polarized Ni electrodes injecting from the bottom Au electrode

Figure S2.2 is the homologous one of Fig. 3 (main manuscript), where the current is now being injected to the helical backbone from the non-polarized Au electrode. The single-molecule histograms show a specular image of that in Fig. 3, demonstrating that inverting the direction of the current flow and keeping all other parameters constant has the same effect but the conductance order is inverted with respect to the Ni magnetic polarization. This behavior can be explained within the same model framework, considering an inversion of the helicity state between both cases (positive bias in Fig. 3 and negative bias in Fig. S2.2). In the new scenario (Fig. S2.2), the spin selected at the Au electrode/peptide interface is compatible with the down magnetic polarization of the top Ni electron-drain electrode. The opposite case presented in the main manuscript provides larger spin filter effect (Fig. 3b) as compare to the optimum case in here (Fig. S2.2a) because the current injected from the polarized Ni electrode in the former is strongly spin-polarized as opposed to the case considered here.

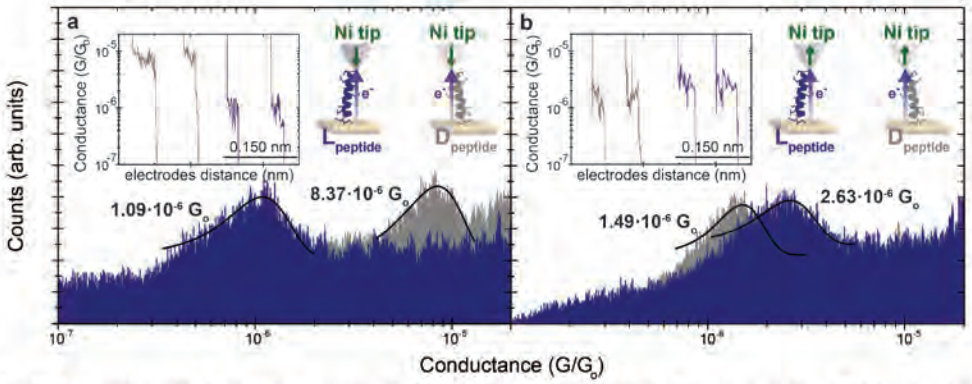

Fig.S2.2 Semilog conductance histograms for the dextrorotatory and levorotatory α-22AA-peptides, under a negative sample bias voltage of -50 mV and using a magnetically polarized Ni tip.

3. Semi-quantitative theory validation and consistency of results

One can check for the consistency of the theory by extracting the values of the ratio of the DOS in the Ni tip and the spin-charge bias using the ratios of the conductance values for both current directions. Given the hierarchy of conductances in Fig.3, the ratio of G_1/G_3 and G_2/G_4 (with $G_1 > G_2 > G_3 > G_4$) give the minority/majority spin ratio at the Ni electrode. Using values in Fig.3: $G_1/G_3 \sim 3.68 \sim g_{Ni}^m / g_{Ni}^M \sim G_2/G_4 \sim 4.08$, representing g_{Ni}^m *and* g_{Ni}^M the DOS of the Ni near the Fermi level for the minority and majority spin charge carriers respectively. On the other hand, the ratios of G_1/G_2 and G_3/G_4 yield the spin-charge voltage; $G_1/G_2 \sim 2.25$ and $G_3/G_4 \sim 2.49$ implying $\mu_{sN} \sim 19$mV and ~21 mV respectively. Both results are very consistent with the conclusions exposed in the main manuscript and in the literature on DOS for Ni.

4. Sample preparation and measurements conditions for the transport measurements

α-22AA-peptides were obtained with acetamidomethyl (*Acm*) as protecting group to prevent the adsorption of peptides through Cys residue.[5–8] Thus, the molecules adsorb on gold using the free thiol group at the C-terminus (cysteamine linker) resulting in a uniform orientation with the C-terminus located near the substrate and the N-terminus exposed at the surface.[5] All glassware and PFTE STM-cells were cleaned with piranha solution (3:1 H_2SO_4/H_2O_2 by volume) before usage followed by rinsing with 18 MΩ cm^{-1} Milli-Q water (Millipore).[9] Ni tips were prepared by mechanically cutting polycrystalline Ni wire (99.99%, Goodfellow, UK). To avoid the Ni wire oxidation under ambient conditions, the prepared Ni tips were magnetically polarized and stored under in anaerobic conditions before use,[10] then were electrically insulated with Apiezon wax. An Au (111) single crystal substrate (10 mm x 1 mm) of 99.9999% purity and orientation accuracy < 0.1 degrees was purchased from MaTeck (Germany). Before each experiment, the single crystal Au (111) substrate was electropolished to eliminate possible residual contamination and then annealed with a H_2 flame. The surfaces were immediately placed in 200 μM α-22AA-peptide solution of 6:4 H_2O/ trifluoroethanol (TFE) (by volume) for 24 h, since it is well known that such mixtures stabilize the helical conformation of

the peptide. To remove de *Acm* group, the modified Au(111) substrate was rinsed with the Milli-Q water/TFE solution and dried in an Ar stream, and immersed in a 15% acetic acid Milli-Q water solution plus 4 eq. of freshly prepared 0,1 M I_2 methanol solution for 24 h at 4°C conditions.[11] Finally, to stop the oxidation, the surface was washed with Milli-Q water and immersed in 0,1 M sodium thiosulfate ($Na_2S_2O_3$) Milli-Q solution for 10 minutes.[11] The Modified Au(111) substrate with the attached deprotected α-22AA-peptides was then introduced in the STM cell that was filled with a 80µL of the Milli-Q water/TFE solution to keep the helicity of the α-22AA-peptides.

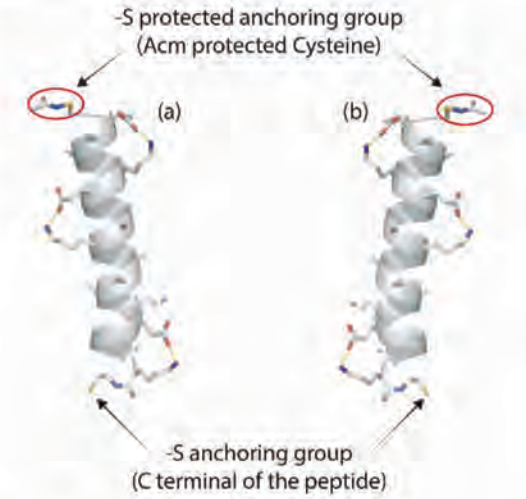

Fig.S4.1 Representation of the dextrorotatory (a) and levorotatory (b) "Acm-thiol protected cysteine" α-22AA-peptides and the amino acid sequence.

5. Solid-phase synthesis and purification of α-peptides

Instrumentation:

HPLC chromatograms were recorded on a Waters Alliance 2695 separation module equipped with a Waters 2998 photodiode array detector and Empower software (Waters) using a Sunfire C_{18} column (100 mm x 4.6 mm, 3.5 µm; Waters); flow: 1mL/min, solvents H_2O (0.045% TFA) and ACN (0.036% TFA).

HPLC-MS were recorded using a Waters Alliance 2695 equipped with a Waters 2998 photodiode array detector, ESI-MS micromass ZQ (Waters) and Masslynx software (Waters) using a Sunfire C_{18} column (100mm x 2.1 mm, 3.5 µm, Waters); flow rate: 0.3 mL/min, solvents H_2O (0.1% formic acid) and ACN (0.07% formic acid).

MALDI-TOF mass spectra were obtained using a MALDI-TOF Applied Biosystem 4700 with a N_2 laser of 337 nm. Matrix: 20 mg/mL α-cyano-4-hydroxycinnamic acid (ACH) in 50%/ 49.9% H_2O/

0.1% TFA. Sample preparation: a mix of 1µL of matrix and 1µL of peptide solution was placed on a MALDI-TOF plate and dried by air.

Peptides were purified by semi-preparative HPLC on a Waters 2700 Sample Manager equipped with a Waters 2487 dual λ absorbance detector, a Waters 600 controller, a Waters fraction collection II and Millenium chromatography manager software (Waters) using a Symmetry C_{18} column (100 mm x 19 mm, 5 µm; Waters); flow: 15 mL/min, solvents H_2O (0.1% TFA) and ACN (0.1% TFA).

Peptide synthesis and characterization:

Syntheses were performed at a 100 µmol scale using a Liberty Blue (automatic synthesizer, CEM). Liberty Blue reaches work temperatures around 90ºC because it is equipped with a microwaves system, which is used in the steps of coupling and deprotection. After de last N-deprotection, the acetyl was introduced using 50 eq DIEA and 50 eq Ac_2O in DMF for 90 minutes at room temperature.

For the cleavage from the resin and removal of protecting groups, the peptidyl-resin was washed with DCM and dried by suction. It was transferred to a 50 ml centrifuge tube and cleavage cocktail was added. The cocktail was composed of 95% TFA, 2.5% TIS and 2.5% H_2O and was chosen to avoid traces of thiols, which can be harmful in conjugation steps. It is left under stirring at room temperature. After 2 hours the solution was evaporated with N2. Separation was done using cold *tert*-butyl methyl ether and centrifugation at 3600rpm and 4°C during 5 minutes. This step was repeated three times. The peptide was dissolved in H_2O / ACN 1:1 and transferred to a centrifugal tube by filtering the solution. It was frozen with liquid nitrogen and it was lyophilized.

D-peptide:

Sequence: Ac-C(Acm)EAAAKEAAAKEAAAKEAAAK-NH-CH_2-CH_2-SH; Side chain protecting groups: Cys(Acm), Glu(tBu), Lys(Boc); Resin: Cysteamine 4-methoxytrityl resin, MW: 2174 Da; HPLC t_R (min, G 0-100% ACN in 8 min): 3.834; HPLC t_R (min, G15-25% ACN in 8 min): 4.228; HPLC gradient used to purify: 15-25% ACN; Purity (%): >99%; MALDI-TOF, $[M+H]^+_{exp}$: 2175.3 Da

L-peptide:

Sequence: Ac-C(Acm)EAAAKEAAAKEAAAKEAAAK-NH-CH_2-CH_2-SH; Side chain protecting groups: Cys(Acm), Glu(tBu), Lys(Boc); Resin: Cysteamine 4-methoxytrityl resin, MW: 2174 Da; HPLC t_R (min, G 0-100% ACN in 8 min): 3.823; HPLC t_R (min, G15-25% ACN in 8 min): 4.349; HPLC gradient used to purify: 15-25% ACN; Purity (%): 90%; MALDI-TOF, $[M+H]^+_{exp}$: 2175.1 Da

6. Technical details of the single-molecule transport measurements

Details about the STM-BJ approach are published.[1,12] All the conductance measurements were carried out with a mechanically and electronically insulated PicoSPM I microscope head controlled by a Picoscan 2500 electronics (all from Agilent) and using a homemade PTFE STM cell. Data captures were acquired using a NI-DAQ_{mx}/BNC-2110 National Instruments (LabVIEW data acquisition System) and analyzed with LabVIEW code. The procedure of a

typical break-junction experiment is based on bringing the STM tip to tunneling distance over a flat clean Au (111) surface area as a first step. The STM feedback is then turned off and the tip is driven into and out of contact with the substrate at a speed of 4-8nm/s. This 2-points feedback loop is used to collect thousands of current decays (5000-6000). Single molecule conductance (G) was determined using the expression $G=I_{step}/U_{BIAS}$, where I is the current and U is the voltage difference (bias) between the two junction electrodes. The current decays are accumulated to semi-logarithmic conductance histograms. The observed plateaus in the individual current decays result in the observed peaks in the conductance histograms and provide an averaged value of the single-molecule conductance. Transient curves that are either noisy or that showed smooth exponential decay because of the absence of molecular bridge formation were rejected when building the histograms using an automatic selection procedure driven by a code written in LabVIEW. The histograms were compiled by applying the same automated selection criteria to each set of the recorded decay curves. The selection procedure allows current traces showing counts exceeding a defined threshold to be added to the conductance histogram. The percentage decay curves that showed clear molecular steps were typically 8–15 % and were all selected for building the histograms. This selection process made peaks in the conductance histograms more prominent above the tunneling background and also allowed a quantitative measurement of the yield of molecular junction formation.

Magnetically pre-polarized Ni tips for the spin-dependent transport experiments were prepare as follow: a freshly cut Ni tip was magnetically polarized *ex situ* by placing it in close proximity to a 1 T NdFeB magnet for a period of 2 hours. After the magnetization, the Ni tip was placed into the STM tip holder. The magnitude and direction of the magnetic polarization of the Ni tip were characterized before and after the STM break-junction experiment using SQUID magnetometry to assure that the Ni magnetization persisted over the entire timeframe of the experiments (see ref [8] from the main manuscript). To avoid the Ni wire oxidation during the polarization process and transport measurements under ambient conditions, the prepared Ni electrode was magnetically polarized and stored in strict anaerobic conditions before use. The Ni tip oxidation has been monitored during use by *ex situ* SEM-EDS electric microscopy (see ref [8] from the main manuscript). Once the tip is transfer to the STM cell, it is driven several times towards the Au surface to get a light Au coating that protects the tip apex surface against further oxidation throughout the timeframe of all the single-molecule transport experiments.

7. References

1. Xu, B. & Tao, N. J. Measurement of single-molecule resistance by repeated formation of molecular junctions. *Science* **301,** 1221–3 (2003).

2. Hines, T. *et al.* Transition from tunneling to hopping in single molecular junctions by measuring length and temperature dependence. *J. Am. Chem. Soc.* **132,** 11658–11664 (2010).

3. Venkataraman, L., Klare, J. E., Nuckolls, C., Hybertsen, M. S. & Steigerwald, M. L. Dependence of single-molecule junction conductance on molecular conformation. *Nature* **442,** 904–7 (2006).

4. Scullion, L. *et al.* Large Conductance Changes in Peptide Single Molecule Junctions Controlled by pH. *J. Phys. Chem. C* **115,** 8361–8368 (2011).

5. Sek, S., Swiatek, K. & Misicka, A. Electrical behavior of molecular junctions incorporating alpha-helical peptide. *J. Phys. Chem. B* **109,** 23121–23124 (2005).

6. Biosystems, A. Cleavage, Deprotection, and Isolation of Peptides after Fmoc Synthesis. *Tech. Bull.* 1–12 (1998).

7. Giralt, E., Albericio, F., Pedroso, E., Granier, C. & van Rietschoten, J. Convergent solid phase peptide synthesis. II. Synthesis of the 1–6 apamin protected segment on a NBB-resin. Synthesis of apamin. *Tetrahedron* **38,** 1193–1201 (1982).

8. Veber, D., Milkowski, J., Varga, S., Denkewalter, R. & Hirschmann, R. Acetamidomethyl. A Novel Thiol Protecting Group for Cysteine. *J. Am. Chem. Soc.* **94,** 5456–5461 (1972).

9. Aragonès, A. C. A. C. *et al.* Large Conductance Switching in a Single-Molecule Device through Room Temperature Spin-Dependent Transport. *Nano Lett.* **16,** 218–226 (2016).

10. Aragonès, A. C. *et al.* Highly conductive single-molecule wires with controlled orientation by coordination of metalloporphyrins. *Nano Lett.* **14,** 4751–6 (2014).

11. Vila-Perello, M., Sanchez-Vallet, A., Garcia-Olmedo, F., Molina, A. & Andreu, D. Structural Dissection of a Highly Knotted Peptide Reveals Minimal Motif with Antimicrobial Activity. *J. Biol. Chem.* **280,** 1661–1668 (2005).

12. Chen, F. & Tao, N. J. Electron transport in single molecules: from benzene to graphene. *Acc. Chem. Res.* **42,** 429–38 (2009).

4.4 Findings and Discussion

— *The main findings of this study were the following:*

- Employing non-magnetized Ni tip electrodes, D- and L- α-22AA-peptides did not show any conductance change between them. From the performed experiments employing Au electrodes for D-α-22AA and 17 AA peptides have been determined a difference of an order of magnitude between both lengths, being the shorter the most conducting.

- Employing magnetized Ni tip electrodes, under the *Ni tip-to-Au substrate* current sense scenario, the α-22AA-peptides showed the two higher conductances were "$L_{peptide}$ with ↑Ni" and "$D_{peptide}$ with ↓Ni ", being the former the larger one. The two lowest conductances corresponded to the "$L_{peptide}$ with ↓Ni" and "$D_{peptide}$ with ↑Ni ", being the former the larger one. The results under the inverted *Au substrate-to-Ni tip* current sense showed a parallel scenario inverting the conductance roles of the $D_{peptide}$ and $L_{peptide}$ chiralities as well as inverting the conductance differences for each Ni tip magnetic polarization. The four conductance scenarios for each current sense were distributed over an order a magnitude range.

- The calculated *spin-polarization power* for each chirality, understood as the asymmetric factor between the current flowing through a peptide with the same chirality but under opposite Ni tip polarizations, was significant similar to the experimental results, being a SP=60% for the $L_{peptide}$ and SP=57% for the $D_{peptide}$.

— *The discussion of the results is summarized below:*

- Can be assumed a coherent tunneling mechanism through a preserved α-helical conformation of the target α-peptides used in the study, because the obtained *β value* (2.7 nm^{-1}) is in agreement with previously reported similar values for equivalent peptide structures.[313,534]

- The obtained conductance differences for D-α-22AA between the junctions employing Ni and Au tip can be attributed to the different used metal, effect previously observed in "*Chapter* ***Fundamental study: Metal complexes***" (discussed on Page 95) and in previous works.[62,197,332,333,335]

- The conductance difference between chiral peptides under non-polarized current is inexistent, they only can show different conductance behavior under polarized current due the spin-polarization. These spin-dependent capabilities of the peptides are closely related to state *helicity* rather than electronic spin, it means that instead of presenting dependence merely on the polarization of the carriers similarly to the Ni tip, the studied paramagnetic complexes or the Spinterface, the filtering mechanism (see *Expression 4.5*, on Page 219) depends

on projection of the spin vector in the direction of propagation, i.e is not only the result of spin-polarization, but also the current sense. For the studied systems, the positive *helicity* (aligned parameters) is the preferred state for $L_{peptides}$, and the negative *helicity* (antialigned parameters) is the preferred state for $D_{peptides}$. For these reasons the conductance roles associated to each peptide chirality can be inverted according to the current sense.

- Under the four *Ni tip-to-Au substrate* current sense scenarios, the polarized electrons are injected from the Ni tip (as *minority* carriers) to the α-22AA-peptides. "$L_{peptide}$ under ↑Ni" as well as "$D_{peptide}$ under ↓Ni" showed the highest conductance scenarios for each chirality. Both scenarios correspond to the transmission of preferred spins through the peptide due the favorable injected spin-carriers population for their chirality, being spin-down for the $L_{peptide}$ (positive *helicity*) and spin-up for the $D_{peptide}$ (negative *helicity*); between both scenarios the conductance differences are due the Spinterface *minority* spin-carriers preferences for the injected electrons from the peptides, consequently $L_{peptide}$ under ↑Ni" junction is the most conducting case. The less conducting scenarios "$L_{peptide}$ under ↓Ni" and "$D_{peptide}$ under ↑Ni "correspond to the transmission of unpreferred spins through the peptide due the unfavorable injected population of spin-carriers for their chirality; between both scenarios, again the conductances differences are caused due the Spinterface *minority* spin-carriers preferences, being the $L_{peptide}$ under ↓Ni" the most conducting case.

- For the four *Au substrate-to-Ni tip* scenarios the interplay between Spinterface, peptides and Ni tip define the same conductance hierarchy presented by the *Ni tip-to-Au substrate* current sense, but inverting the conductance roles associated to each peptide chirality as a consequence to their opposed *helicity* preferences due the inversion of the current sense. In this case the electrons are selected on the peptide and injected to the Ni tip. The electrons selection is defined due the preferred spins by the peptides supported by their chirality, being the emitted electrons spin-up for the $L_{peptide}$ (positive *helicity*) and spin-down for the $D_{peptide}$ (negative *helicity*). When such polarized electrons are injected to the Ni tip electrode only the *minority* spin population will be favorable transmitted, this defines the two scenarios of high conductances regimes "$D_{peptide}$ under ↓Ni" and "$L_{peptide}$ under ↑Ni", as well as the two low conductances regimes "$D_{peptide}$ under ↑Ni"and "$L_{peptide}$ under ↓Ni". Inside each scenario of high or low conductances regime, the final conductance is tunned again via the Spinterface *minority* spin-carriers preferences over the injected polarized-current.

- Even the performed experiments were done employing an asymmetric junction, the effects of the current inversion is not affecting the spin-dependent current behavior because the predominant effects are the interplay between the Ni tip and *helicity* spin preferences, and both can present and can invert their source and drain roles.

4.5 Conclusions of the Chapter

In this Chapter is established for the first time a single-molecule device based on α-helical peptides junctions used to verify and determine the electronic spin filtering capabilities at RT of chiral systems based on the CISS effect. In order to study it, were performed single-molecule current measurements employing the STM-BJ technique via the robust and stable asymmetric junctions of the peptide between a polarized ferromagnetic Ni tip and a Au substrate electrodes. The main differences presented on this Chapter regarding the previous studied single-molecule devices, are the use of diamagnetic molecules and the novelty to tune the current via two different stimuli: the chirality of the molecule and the Ni tip magnetic polarization direction.

As a main conclusion, can be deduced that the obtained results are successfully consistent with the proposed modified Landauer transport theory, by the imposed spin-polarization effects of the selected key-parameters: the magnetic peptide-Au Spinterface, the magnetic Ni tip magnetic polarization direction and the peptide chirality. All of them were efficiently incorporated to the experimental *set-up* via three controlled parameters: like the current sense due the applied bias voltage, the spin selectivity of the chiral molecule (through its chirality) and the (*ex-situ*) magnetic polarization of the Ni tip.

From the observed phenomenology can be extracted as a main conclusion that the junction conductance depends on two different energy penalties for the polarized electrons, consequence of the interplay between the transported electrons and the key-parameters' spin-carrier preferences. The first penalty is the consequence of the spin-preferences of both Ni tip ***magnetic polarization*** and peptide's chirality for the electrons transported between them. Indistinctly of the current sense, one of these two components always will inject selected spin-carriers to the other, and the spin preferences of the latter will favor or withdraw the injection of polarized electrons, affecting to the current. The second penalty is applied to the transmitted electrons through the peptide-Au Spinterface, because the interplay between the electrons' polarization and the Spinterface's spin preferences will tune the current. Thanks to these two penalties and their combination can be explained for both current senses, the four observed scenarios with different molecular conductance, as well as determine the qualitative contribution of each penalty. The major filtering effect over the conductance imposed by the energy penalty due the interplay between the peptide's *helicity* and Ni tip, splits the four scenarios in two cases of high and low conductance ranges where the injected polarized electrons are favored or withdrawn, respectively. Inside each current case, the junction conductance is finally tuned due the contribution of the less significant penalty which depends on the interplay between the transported electron spin-polarity and the Spinterface, it splits again each case in two conductance differentiated regimes due the favored or unfavored injection through the Spinterface. The weakness of the penalty with the minor role is due the Spinterface by itself, because it lacks on an effective polarizing character for the current because of using diamagnetic peptides instead of paramagnetic molecules.

Under these conditions, the Rashba spin-splitting of the Au surface is not enhanced due the absence of the paramagnetism unlike the previous Chapters, and as a consequence the current transmitted through the S-Au Spinterface is not filtered, despite being slightly tuned as a consequence of the mentioned penalty. Otherwise, only two scenarios could be possible from the four observed experimentally, because the cases under an effective penalty instead of reducing the conductance the current should be totally filtered like in previous Chapters 2 and 3. Although the Spinterface polarizing effect is weak in comparison to the studied previously, the Ni tip is not able to flip it magnetization direction due its massive superficial extension compared with the Ni tip, otherwise it invalidates two of the four observed scenarios, again.

A part form the exposed main conclusion, others list below as a corollary of all the presented work on this Chapter.

- The observed behavior for the presented single-molecule device allows to tune the current in different conductance levels, close to the observed on Chapter 3, thus behaves more like a Spintronic "variable resistor" than a switch, allowing to control four conductance levels through changing only two parameters like the Ni tip orientation and chirality. Such double control mechanism, much like a spin-valve, offers a improved current signal modulation compared to the switching behavior offered by such spin-valves, which in addition present lower GM ratios.

- The employed peptides present asymmetries not only in terms of the chirality/*helicity*, also they present a structural asymmetry in the oligopeptidic *porphyrin ring* terminations due the different used (*anchoring groups*), it arises an inherent dipole moment along the molecular axis.[536] This dipole can induce another asymmetry to the system[537] and thereby could be used as a new *key-parameter* if the orientation of the molecule-electrode junction attachment is controlled. In the presented study, the orientation and its dipole are kept to a fixed position, so is not affecting to the observed spin-dependent effects on electronic transport. However, despite the dipole moment is not biasing the results because is a common effect for all the studies cases, its contribution can be enough significant to enhance globally the Rashba splitting and consequently the Spinterface effect.[153,201,287,538]

- The achieved conductance modulation thanks to combine the peptide chirality and the Ni tip polarization is up to one order of magnitude range, equivalent to the obtained shorting the electron-pathway ca. 0.8 nm due the peptide length reduction from 22-AA to 17-AA. This attests the significant role of the transmission tunneling barrier's energy modulation, because the consequences of lowering or growing it directly tune the measured molecular conductance increasing or reducing it respect the obtained value under non-magnetized Ni electrodes.

- These new insights contribute to the electron transport research field and especially to the electron transfer in biological systems due the employed molecules'

nature, providing new information about the transmission tunneling barriers in molecular structures allowing to use such structures in molecular circuitry with the added value of the spintronic offered capabilities. In addition, the spin-dependent conductance effects showed by α-22AA-peptides are in the limit of zero voltage conductance therefore operating under effective small currents ranges, it highlights the molecular origin of the effect and the associated low power consumption of the single-molecule device and its potential benefits to incorporate it future devices, similarly to the presented by the devices studied on the previous Chapters.

- The implications of this research allow the CISS to be used as a basis to build spin-filter devices with a more extended application field than the offered by the previous studied metal complexes and *nanoscale*, due their significant drawback since the several physical and chemical requirement which they have to gather to present spin-filtering capabilities.